Proceedings of the 21st ICSMGE, Vienna, Austria, 14 – 19 June 2026. Pistrol, Adam & Schweiger (eds.)
Published by: ÖGG, Austrian Society for Geomechanics, Salzburg, Austria, ISBN 978-3-9503898-4-5
https://doi.org/10.53243/ICSMGE2026-1140

Discrete Modeling of the Internal Fabric of Volcanic Scoria

Juárez-Orta, José Armando
Posgrado de ingeniería, Universidad Nacional Autónoma de México, México, ing.juarezorta@hotmail.com

Jesús Sánchez Guzmán
Associate professor, Facultad de Estudios superiores Aragón, Universidad Nacional Autónoma de México, México

Gabriel Auvinet Guichard
Research professor, Instituto de Ingeniería, Universidad Nacional Autónoma de México, México

ABSTRACT: This study presents the simulation of the internal fabric of volcanic scoria, known in Mexico as *tezontle*, using the Discrete Element Method (DEM). This volcanic scoria with its highly porous and granular nature requires precise modeling to understand its behavior. DEM simulations were conducted to evaluate porosity, contacts distribution, pore size distribution and the effect of grain size distribution on structural properties. Grains with sub-spherical-sub-angular shapes were modeled using the Linear Contact Model with rolling resistance. Surface roughness and angularity could be reproduced using a friction coefficient of 0.7 and a rolling resistance coefficient of 0.6. The representativeness of the simulated samples was validated through the standard deviation of the local porosity. The effect of grain size distribution was analyzed. Results show that well-graded samples exhibit greater particle segregation compared to poorly graded ones. Pore size distribution analyses revealed average pore sizes of 0.012 and 0.15 times the maximum grain size for well-graded samples and for poorly graded samples, respectively. Contact distribution analyses showed a high concentration of contact points at the poles of grains, regardless of grain size distribution. This suggests that particle grading does not affect contact distribution but strongly influences pore structure. These findings provide valuable data on the inner structure of volcanic scoria and demonstrate the potential of DEM to model granular materials.

KEYWORDS: DEM, Volcanic scoria, rolling resistance, inner structure

1 INTRODUCTION

The volcanic scoria originates as magma rises toward the surface, where a reduction in pressure causes the internal gas to escape. This process results in a porous structure, irregular grain shape and variable particle size. The material is lightweight, typically exhibiting red or black coloration and a minerology composition similar to basaltic and andesitic rocks (Pirsson, 1947). Volcanic scoria cones form during one or multiple eruptive events. In Mexico, this volcanic scoria is named *Tezontle*, a term of Nahuatl origin (Tetl: stone, tzontli: hair). The granular material derived from this rock possesses advantageous physical properties that have encouraged its use in industrial construction applications (Rodríguez 2011; Harker & Mahar, 2013; Hossain, 2004 and Hermann *et al.,* 2017). In geotechnical applications, understanding its mechanical behavior is essential. Some studies have explored the physical and mechanical properties of this material (Sabatan *et al*., 2000; Agustin & Goto, 2008; Chávez & Arreygue, 2011; Mendoza, 2021), the available data remain limited. Therefore, it is of interest to investigate this material through an approach that considers structural characterization at the particle level which is difficult to evaluate though conventional laboratory testing.

The Discrete Element method (DEM) proposed by Cundall & Strack (1971) has been important in the study of granular materials. It is widely used for simulating granular materials, allowing study of its structure internal and micromechanical behavior. Auvinet & Sánchez (2023) have studied the internal fabric and mechanical behavior of granular materials by means of probabilistic and computational models.

This paper provides a study of the internal fabric of a volcanic scoria sample, using the DEM and the concepts proposed by Auvinet & Sánchez (2023).

2 CHARACTERIZATION OF A VOLCANIC SCORIA

The granular material is found in the area surrounding Mexico City and exhibits a grain size distribution (GSD) characterized by a uniformity coefficient (C_u=2.98), curvature coefficient (C_c=1.05), and minimal (D_{min}=2.00 mm) and maximal grain size (D_{max}=19.05 mm). In this study, volcanic scoria was analyzed using two grain size distributions: the natural distribution (sample 1) and a hypothetical distribution (sample 2) designed to meet typical specifications for geotechnical materials used as subbase under a roadbed (Mendoza & González, 2016) (Figure 1). Table 1 summarizes the characteristics of both GSD.

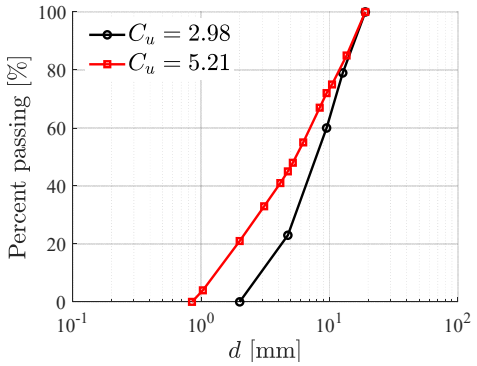

Figure 1. Grains size distributions of a volcanic scoria sample

Table 1. Characteristics of grain size distributions

Sample	D_{min}	D_{max}	D_{max}/D_{min}	C_u	C_c
1	2.00	19.05	9.53	2.98	1.05
2	0.85	19.05	22.41	5.21	0.87

The geometrical characteristics of the grains were evaluated based on the concept of sphericity and angularity. The expressions (1) and (2) proposed by Wadell (1932), and the computational method developed by Zheng & Hryciw (2005) were applied for quantitative analysis. Grain classification was

conducted according to the criteria suggested by Krumbein & Sloss (1951), which incorporate both sphericity (S) and angularity (A) parameters (Figure 2 and Figure 3).

$$S = \frac{D_a}{D_c} \quad (1)$$

$$A = \frac{\sum \frac{r_i}{R}}{N} \quad (2)$$

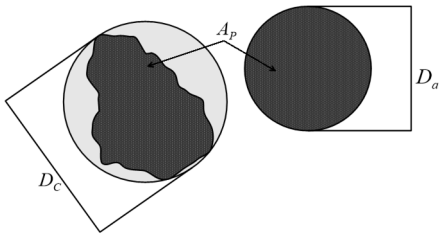

Figure 2. Schematic representation of the sphericity measurement procedure (Zheng & Hryciw, 2005)

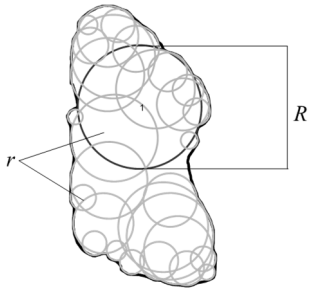

Figure 3. Schematic representation of the angularity measurement procedure

where:
S: sphericity
D_a: equivalent diameter corresponding to the grain's surface area projected on a plane
D_c: diameter of the circle that encloses the projected surface of the particle on a plane
A_p: equivalent circular area corresponding to the grain's surface area projected on a plane
A: angularity
r: radius of the circle tangent to the concave vertices of the projected particle outline
R: radius of the maximum inscribed circle within the planar projection of the particle surface
N: number of circles tangent to the concave vertices of the projected particle outline

S and A were evaluated for thirty grains from each fraction of the grain size distribution. For each grain, a digital image of its projected surface on a plane was obtained, as required by the computational method proposed by Zheng & Hryciw (2015). Figure 4 shows the projected surface of some grains on a plane, which were used to determine their sphericity and angularity. The mean values of sphericity and angularity were 0.81 and 0.26, respectively. According to the classification by Krumbein & Sloss (1951), these values indicate that the grains in the volcanic scoria sample present a sub-spherical to angular morphology, which is consistent with the findings by Zhihong *et al*., (2021).

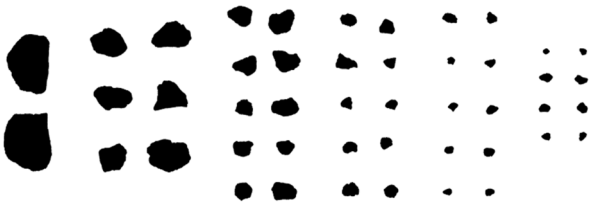

Figure 4. The projected surface of several grains on a plane

The porous structure of grains contributes to a relatively low density. Grain density (Gs) was measured using the paraffin method (ASTM C127-88), applied to selected samples from each grain size class. The mean Gs value obtained was 1.78, which is higher than the values reported by Hossain (2004), McGetchin *et al.,* (1974), Sabtan & Shehata (2000) and Mendoza (2021). However, it is comparable to the values obtained for volcanic scoria found in Indonesia and Yemen, as reported by Al-Akhaly & Al-Sakkaf (2020).

The angle of repose (AR) of volcanic scoria cinder cones is influenced by volcanic activity. According to Blake (2021), cinder cones rarely exceed 300 m in height and 900 m in diameter, exhibiting slope angles of approximately 33º. Cas & Wright (1988) mentioned that cinder cones are composed of a loosely consolidated material susceptible to erosion. Therefore, youngest cinder cones achieve slope angles ranging from 30º a 35º and older cinder cones present slope angles as low as 15º.

Considering the above, the AR of the volcanic scoria sample was measured in laboratory. The experiment was conducted using a representative setup, employing the cylindrical vessel pouring method (Beakawi & Baghabra, 2018). The grain size distribution used was that of sample 1, as it corresponds to volcanic scoria deposit (Figure 1). Figure 5 shows the measured AR of volcanic scoria sample. This sample achieved an angle of repose equal to 31º.

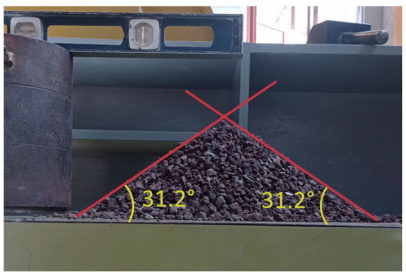

Figure 5. Angle of repose of a volcanic scoria sample

3 DEM PARAMETER

DEM simulations of volcanic scoria samples using the Rolling Resistance Linear Contact Model (RRLCM) were performed. RRLCM incorporates a friction coefficient (μ_f) and rolling resistance coefficient (μ_r), which allows representing surface roughness and angularity (Jun *et al.,* 2011), respectively.

Several studies have employed angle of repose simulations to calibrate parameters in DEM models. Alizadeh *et al*., (2018) conducted both experimental and numerical measurements of AR using the fixed funnel method. Auvinet & Sánchez (2020) performed cylindrical vessel pouring simulations to determine parameters μ_f and μ_r of a volcanic scoria sample.

Angle of repose simulations were performed to calibrate parameters for DEM models of the volcanic scoria sample. The methodology proposed by Itasca (2015) was employed, which consists in performing DEM simulation based on the cylindrical vessel pouring method. The process consisted of three stages: placement of material into a cylindrical vessel, pouring of the

vessel contents and measurement of the angle of repose (Figure 6). The GSD with C_u=2.98 was used, as it corresponds to volcanic scoria deposit (Figure 1). The stiffness of the contact between grains was calculated employing the expressions proposed by Potyondy & Cundall (2004) which are in function of elasticity modulus (E_c) of the particles. Bell (1983) suggests E_c= 5x10^{10} [Pa] for highly porous rocks.

A parametric analysis was performed considering values of μ_f and μ_r ranging from 0.4 to 0.8 and 0.1 to 0.9, respectively. Figure 6 shows the cones formed under different combinations of μ_f and μ_r. Figure 7 presents the variation of *AR* under different combinations of μ_f and μ_r. The results indicate that the value of *AR* is proportional to μ_r. The numerically obtained *AR* values fall within the range of μ_f from 0.4 to 0.8. Following Cambou (1974), this range was restricted to 0.5-0.8. The μ_r values ranged from 0.4 to 0.9.

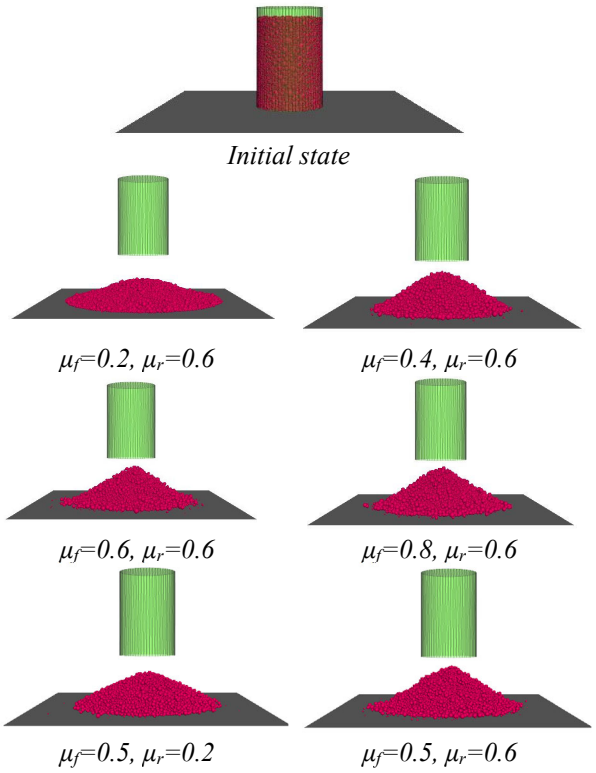

Figure 6. Cones formed for different combinations of μ_f and μ_r

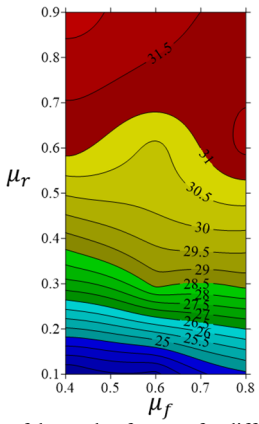

Figure 7. Variation of the angle of repose for different values of μ_f and μ_r

Based on the above results and the observations of Cas & Wright (1988) and Cambou (1974), values of μ_f=0.7 and μ_r=0.6 were adopted (Figure 7). They are consistent with the findings of Auvinet & Sánchez (2020).

4 FABRIC OF VOLCANIC SCORIA

DEM simulations of cubic specimens of volcanic scoria were performed using the GSD shown in Figure 1. The dimensions of each specimen were 30 cm in height and 30 cm in width. The specimen, with a C_u= 2.98, required 70,000 particles to reproduce grains size distribution, while sample with a C_u=5.21 required 90,000 particles. RRLCM was employed to represent particle interaction. Normal and shear stiffness values were set to 1x10^7 N/m, and μ_f=0.7 and μ_r=0.6 were adopted. Figure 8 presents a comparison between numerically and experimentally obtained GSD; a good fit is observed in both cases.

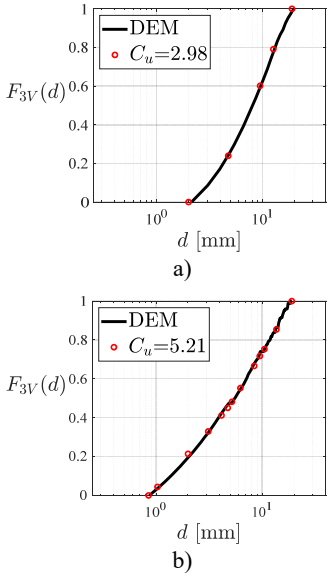

Figure 8. Comparison between the numerical and experimental GSD a) sample 1 b) sample 2

4.1 *Porosity*

The porosity of the specimens was evaluated inside the central measurement cube (*cmc*) using the Monte Carlo technique, which involves generating random points in space and recording those that fall within the voids. Auvinet & Sánchez (2023) recommended using 10^7 or more random points. Porosity (n) was calculated as the ratio of the number of points within the pores to the total number of points. The standard deviation of local porosity was evaluated using the method suggested by Auvinet & Bouvard (1984). These authors propose an expression which is a function of porosity, specific grain surface (S_3) and size of *cmc*:

$$\frac{\sigma_n}{\sqrt{n(n-1)}} = 1.4\left[\frac{aS_3}{4n(1-n)}\right]^{-\frac{3}{2}} \quad (3)$$

where:
σ_n: standard deviation of local porosity
a: edge length of central measurement cube

$$S_3 = \frac{\sum a_s}{\sum V_p} \quad (4)$$

a_s: particle surface area
V_p: particle volume

A sensitivity analysis was performed to evaluate the effect of central measurement cube size. The bias caused by boundary effects was mitigated by maintaining a distance equal to l=2D_{min}

between the specimen borders and *cmc* (Auvinet & Sánchez, 2023). Figure 9 presents the variation of porosity for both samples under different *cmc* sizes. It is observed that as *a* increases, porosity converges toward a stable value.

Figure 10 shows the variation of σ_n for different *cmc*. The results indicate that the effect of *cmc* size is negligible for cube edge lengths greater than $10D_{max}$. The porosity of specimens was estimated using a *cmc* with $a=12D_{max}$. Table 2 presents the characteristics of simulated volcanic scoria specimens. It is observed that both samples exhibit similar porosity values.

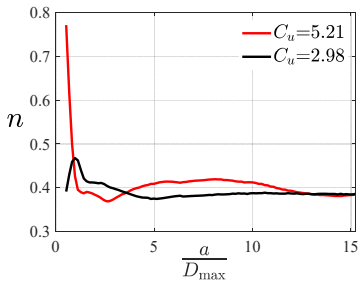

Figure 9. Variation of local porosity for volcanic scoria samples with different *cmc* sizes

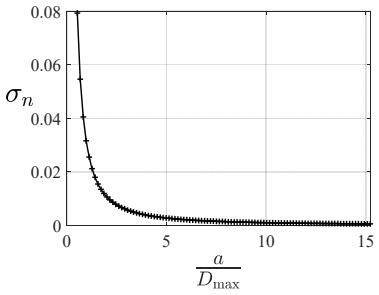

Figure 10. Variation of σ_n for different *cmc*

4.2 *Homogeneity*

Auvinet (1986) proposes the concept of spatial distribution of particles per unit of volume, area and length. This allows describing the array of particles within a homogeneous mass of granular material. The number of grains intercepted by horizontal planes at different heights of the simulated cubic volcanic scoria specimens was recorded. Figure 11 presents the grain proportion along the height of specimens, normalized with respect to minimum particle diameter. The results reveal a higher grain concentration near the bottom of the specimen, a phenomenon known as segregation (Auvinet & Sánchez, 2023). This effect was more pronounced in sample 2 with C_u=5.21, which presented higher values of $D_{máx}/D_{mín}$ and C_u. In contrast, sample 1 with C_u=2.98 exhibited a nearly constant grain proportion per unit area throughout its height. The expected value of particles per unit of area in sample 1 is 6.93×10^4 and in sample 2 is 2.05×10^5.

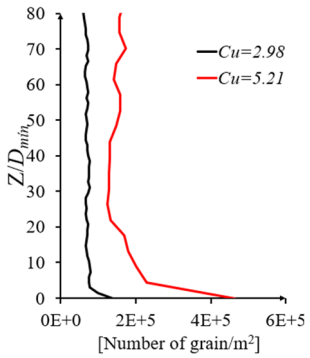

Figure 11. Homogeneity of volcanic scoria samples

4.3 *Coordination number and contacts distribution*

The coordination number $\overline{N_c}$ represents the mean number of contacts per particle. It is widely used to evaluate the packing structure in granular assemblies (Auvinet & Sánchez, 2023).

Oda (1972) and Cambou *et al*., (2009) reported several empirical correlations between $\overline{N_c}$ and the porosity for materials of spherical samples. However, Auvinet & Sánchez (2023) noted that no direct relationship exists between these properties as revelated in Table 2.

The coordination number of volcanic scoria samples was determined. Sample 2 with wider grain size distribution presents a higher $\overline{N_c}$ than sample 1 (Table 2).

Table 2. *n* and $\overline{N_c}$ of a volcanic scoria sample

Sample	$D_{máx}/D_{mín}$	C_u	*n*	$\overline{N_c}$
1	9.525	2.98	0.39	3.83
2	22.41	5.21	0.39	4.27

The concept of "*fabric*" in granular assemblies was proposed by Brewer (1964). It is used to describe the spatial arrangement of solid particles and voids. The position of a contact on the surface of a grain is defined by angles α y β (Figure 12) and the distribution of the corresponding vector is represented by $\Gamma(\alpha,\beta)$ (Auvinet & Sánchez, 2023):

$$\int_{\Omega} \Gamma(\alpha,\beta)d\omega = 1 \qquad (5)$$

where:

Ω: sphere of unit radius
dω: elemental solid angle equal to $cos\alpha d\alpha d\beta$
$\left(-\frac{\pi}{2} < \alpha < +\frac{\pi}{2}; 0 < \beta < 2\pi\right)$

$\Gamma(\alpha,\beta)d\omega$ represents the probability that a normal vector to the tangent plane at the contact points be located in the elemental solid angle (Auvinet & Sánchez, 2023) (Figure 12).

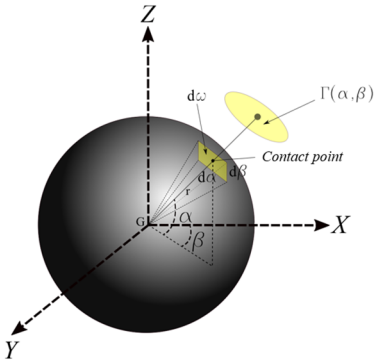

Figure 12. Spatial distribution of contact orientation represented by $\Gamma(\alpha,\beta)$

Auvinet & Sánchez (2023) observed that, in structures deposited under the gravity field, $\Gamma(\alpha,\beta)$ is independent of angle β. Therefore, the function can be simplified as a function $\Gamma(\alpha)$ such that:

$$\int_{-\frac{\pi}{2}}^{\frac{\pi}{2}} \Gamma(\alpha) cos\alpha d\alpha = 1 \qquad (6)$$

If contacts are uniformly distributed over the surface of the grains (geometric isotropy), it can be verified that $\Gamma(\alpha,\beta)=1/4$ and $\Gamma(\alpha)=1/2$. As stressed by Auvinet (1986), deviations from

these reference values indicate the presence of geometric anisotropy.

The distribution of the contacts was evaluated in the simulated volcanic scoria samples. Figure 13 presents $\Gamma(\alpha)$ for each sample. It is observed a high concentration of contacts near the poles of grain surface corresponding to an inherent anisotropy. This is due to friction and roughness on the surface of the grains. No effect of grain size distribution on $\Gamma(\alpha)$ was observed.

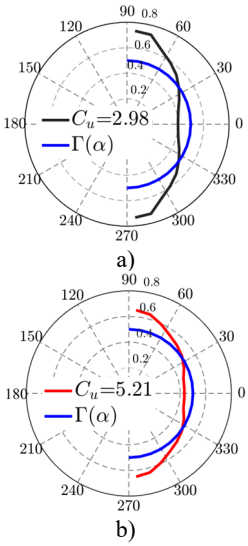

Figure 13. Distribution of contacts on the grain surface for simulated volcanic scoria samples: a) C_u=2.98 b) Cu=5.21

4.4 *Pore size distribution*

The voids formed in a granular media can be studied like individual pores for quantifying its essential characteristics (Auvinet & Sánchez, 2023). Matheron (1967) proposed a function for describing the dimensions of pore ($F_{3V}(p)$). This is the proportion of the total volume of voids inaccessible to a reference sphere with diameter p. The origin of this definition can be found in the so-called Purcell's diagrams obtained from mercury porosimeters by measuring the volume of this metal penetrating inside a sample under different pressures (Auvinet & Sánchez, 2023).

Auvinet (1986) indicates that function $F_{3V}(p)$ does not strictly correspond to the one obtained using Purcell's diagram, since some pores may accommodate the reference sphere but are not accessible to mercury from the exterior due to a lack of entry paths. The pore size probabilistic density is defined as the derivative of the volumetric distribution function:

$$f_{3V}(p) = \frac{dF_{3V}}{dp} \tag{7}$$

To determine the pore size distribution in simulated volcanic scoria samples, the method proposed by Auvinet & Sánchez (2023) was used:

- Random points were generated inside the core of the structure analyzed. The number of points falling outside the grains was recorded. The ratio between this number and the total number of generated points was used to estimate porosity at the same time.
- For each point, a trial-and-error process was used to determine the smaller diameter D of the reference sphere for which the points remained within an inaccessible volume or intersection of such sphere exists with the particles of the medium.
- $F_{3V}(p)$ was estimated as the ratio between the number of points falling inside an inaccessible volume associated with the diameter equal to or smaller than a given value p and the total number of accepted points.

The pore size distribution (PSD) was calculated for the simulated volcanic scoria samples. Figure 14 presents the PSD results for both specimens. Sample 1 exhibits a more uniform $F_{3V}(p)$ distribution compared to sample 2. The results indicate that the average pore size is approximately 0.15 D_{max} for sample 1 with C_u=2.98 and 0.012 D_{max} for sample 2 with C_u=5.21. The largest PSD dispersion is observed in the sample with C_u=5.21 (Figure 15), whereas the smallest PSD dispersion corresponds to sample with C_u=2.98 (Figure 16).

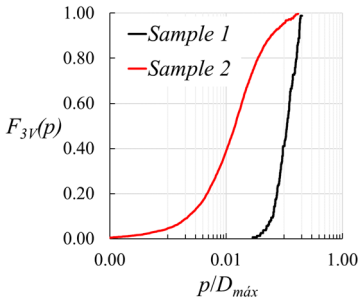

Figure 14. Pore size distribution of simulated volcanic scoria samples

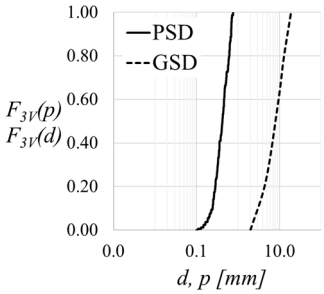

Figure 15. PSD and GSD of sample 1

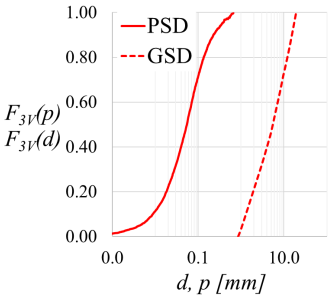

Figure 16. PSD and GSD of sample 2

5 CONCLUSIONS

In this study, DEM simulations of internal fabric of volcanic scoria were performed. The DEM was enabled to reproduce the structure of volcanic scoria samples, using the Rolling Resistance Linear Contact Model. A friction coefficient of 0.7 and a rolling resistance coefficient of 0.6 were applied to account for the effects of surface roughness and angularity of grains.

Several properties of the volcanic scoria structure were evaluated, including porosity, homogeneity, coordination number, distribution of contacts and pore size distribution. The representativeness of the simulated samples was validated through the standard deviation of the local porosity.

It was observed that the porosity is independent of the grain size distribution, as both samples achieved similar values.

The coordination number was slightly higher in well-graded samples, attributed to their wider grain size distribution. The segregation phenomenon was more pronounced in well-graded materials, with higher values of $D_{máx}/D_{mín}$ and C_u. The poorly graded exhibited a nearly constant grain proportion per unit area throughout its height.

The distribution of contacts on the grain surface of volcanic scoria revealed inherent geometric anisotropy with high concentration of contacts near the poles. This property was found to be independent of the grain size distribution.

The pore size distribution of the volcanic scoria samples was determined. The results revealed average pore sizes of 0.012 and 0.15 times the maximum grain size for well-graded samples and for poorly graded samples, respectively.

6 ACKNOWLEDGEMENTS

The authors would like to express their gratitude to CONAHCyT and Institute of Engineering at UNAM for their valuable support throughout the development of this work.

7 REFERENCES

Agustian, Y. and Goto, S. 2008. Strength and deformation characteristics of scoria in triaxial compression at low confining stress", Soil and Foundation Japanese Geotechnical Society, Vol. 48, No. 1, pp. 27-39, February 2008.

Al-Akhaly, I., A. and Al-Sakkaf, A., A. 2020. Assessment of engineering properties of Al-Haweri scoria, NW Sana'a Yemen, Journal of Geological Engineering, 44(2020), pp 117-131, doi 10.2432/jmd.826975.

Alizadeh, M., Asachi, M., Ghadiri, M., Bayly, A. and Hassanpour A. 2018. A methodology for calibration of DEM input parameters in simulation of segregation of powder mixture, a special focus on adhesion", Powder Technology, Volume 339, PP. 789-800, ISSN 0032-5910, https://doi.org/10.1016/j.powtec.2018.08.028.

Auvinet, G. and Bouvard, D. 1984. Effet d'échelle géométrique dans les milieux granulaires. Revue Française de Géotechnique, N°25, 63-69.

Auvinet, G. 1986. Estructura de los medios granulares. Tesis doctoral. División de Estudios de Posgrado, Facultad de Ingenie ría, Universidad Nacional Autónoma de México, México.

Auvinet, G. and Sánchez, J. 2020. Diseño de terraplenes ligeros para control de asentamientos", Ingeniería Investigación y Tecnología, Volumen XXI (número 4), octubre-diciembre 2020 1-9, https://doi.org/10.22201/fi.25940732e.2020.21.4.034

Auvinet, G. and Sánchez, J. 2023. Estructura y micromecánica de medios granulares / Fabric and micromechanics of granular media. Bilingual book published by Instituto de Ingeniería, UNAM and Sociedad Mexicana de Ingeniería Geotécnica (SMIG), Mexico.

ASTM C127-88 Standard test method for density, relative density (specific gravity), and absorption of coarse aggregate, West Conshohocken, PA.

Beakawi Al-Hashemi H., M. and Baghabra Al-Amoudi O., S. 2018. A review on the angle of repose of granular materials, Powder Technology, Volume 330, Pages 397-417, ISSN 0032-5910, https://doi.org/10.1016/j.powtec.2018.02.003

Bell, F. G. 1983. "Fundamental of engineering geology: Mechanical properties of rocks", Butterworth-Heinemann, pp. 488-527, doi.org/10.1016/B978-0-408-01169-3.50015-8.

Brewer, R. 1964. Fabric and mineral analysis of soil, Wiley, New York

Chávez, C. and Arreygue, E. 2011. Caracterización mecánica de la escoria volcánica (tezontle) de la zona de Morelia, Michoacán, México, 2011-Pan-Am CGS Geotechnical Conference.

Cambou, B. 1974. Etude du frottement entre matériaux rocheux. Coopération technique Franco-Mexicaine :Instituto de Inge niería, UNAM, México.

Cambou B., Jean M. and Radjaï F. 2009 "Micromechanics of granular materials", ISTE, John Wiley and Sons.

Cas, R. A. F. and Wright, J. V. 1988. Volcanic Successions: Modern and Ancient-A Geological Approach to Process, Products and Successions, Champman and Hall, London.

Cundall P. A. and Strack O. D. L 1979. A discrete numerical method for granular assemblies, Géotechnique, 29, 47-65

Harker, K. T. and Mahar, J. 2013. Use of porous concrete and scoria bases to clean groundwater recharge, Seventh International Conference on Cases Histories in Geotechnical Enginerring, Chicago, United States, April 29-Mai 4, 2013

Hernann, W., Tchamdjou, J., Grigoletto S., Michel F., Courand, L., Abidi, L. M. and Cherradi, T. 2017. An investigation on the use of coarse volcanic scoria as sand in Portlan cement mortar, Case studies in construction materials, 7, 191-206, http://dx.doi.org/10.1016/j.cscm.2017.07.005

Hickson, C., Spurgeon, T., Tilling R. and Adam, P. 2013. Factors Influencing Volcanic Hazards and the Morphology of Volcanic Landforms, Editor: John F. Shroder, Treatise on Geomorphology, Academic Press, pp. 219-242, https://doi.org/10.1016/B978-0-12-374739-6.00360-2.

Hossain, K. M. A. 2004. Properties of volcanic scoria based lightweight concrete, Magazine of Concrete Research, 56, No.2, March, 111-120

Itasca Consulting Goup Inc. 2015. Particle flow code 5.0, documen tation. Updated Jun, 2019

Huff, W., D. and Owen, L., A. 2015. Volcanic Landforms and hazards, Reference n Earth Systems and Environmental Sciences, Elsevier, https://doi.org/10.1016/B978-0-12-409548-9.09512-9

Jun, Ai., Jian-Fei, C., J., Michael Rotter. And Jin, Y., O. 2011. Assessment of rolling resistance models in discrete element simulations, Powder Technology, Volume 206, Issue 3, Pages 269-282, https://doi.org/10.1016/j.powtec.2010.09.030.

Krumbein, W., C. and Sloss, L., L. 1951 Stratigraphy and sedimentation. San Francisco, USA: W. H. Freeman and Company.

Matheron, G. 1967. Eléments pour une théorie des milieux poreux, Masson et Cie. Editeurs, Paris, France

McGetchin, T. R., Settle, M. and Chouet B. A. 1974. Cinder cone growth modeled after northeast crater, Mount Etna, Sicily, Journal of Geophysical Research, Vol.79, No. 23, pp. 3257-3272.

Mendoza M. J. and González M. D. A. 2016. Shear strength and deformability of volcanic scoria from Mexico City and its surroundings. XXVIII Reunión Nacional de Ingeniería Geotécnica, Sociedad Mexicana de Ingeniería Geotécnica (SMIG). Nov, Mérida Yucatán, México.

Mendoza. M. J. 2021. Tezontles o escorias volcánicas del Valle de México: Génesis, propiedades ingenieriles y usos en construcción, Novena conferencia Raúl J. Marsal Córdoba, Sociedad Mexicana de Ingeniería Geotécnica, A.C (SMIG).

Oda, M. 1972. Initial fabrics and their relations to mechanical properties of granular material, Japanese Society of Soil Mechanics and Foundation Engineering, Volume 12, No. 1, pp 17-37. Tokyo, Japan.

Pirsson, V. L. 1947. Rocks and rocks minerals, Third edition, New York: J. Wiley.

Potyondy, D. O. and Cundall, P. A. 2004. A bonded-particle model for rock, International Journal of rock mechanics & Mining Sciences 41 (2004) pp. 1329-1364.

Rodríguez, L. 2011. La práctica constructiva en la Ciudad de México: El caso del tezontle, siglos XVIII-XIX. Boletín de monumentos históricos. Tercera época, Núm. 22

Sabatan, A. A. and Shehata, W. M. 2000. Evaluation of engineering properties of scoria in central Harrat Rahat Saudi Arabia, Bull Eng Geol Env (2000) 59:2019-225 Springer-Verlag

Wadell, H. 1932. Volume, shape and roundness of rock particles, The journal of geology, Vol. 40, No. 5, pp 443-451.

Zheng, J. and Hryciw, R., D. 2015 Traditional soil particle sphericity, roundness and surface roughness by computational geometry, Géotechnique, vol. 65, N° 6, pp. 494.506, Doi:10.1680/geot/14-P-192.

Zhihong, N., Qun, Q. Xiang, W., Zhengyu, L. and Aijun, A. 2021. Shape quantification of volcanic cinders and the influence of particle shape indexes on accumulation characteristics, International Journal of Pavement Engineering, doi: 10.1080/10298436.2021.2001816.